Journal of Plankton Research Vol.20 no.8 pp.1615–1636, 1998

Feeding, prey selection and prey encounter mechanisms in the heterotrophic dinoflagellate *Noctiluca scintillans*

Thomas Kiørboe and Josefin Titelman

Danish Institute for Fisheries Research, Charlottenlund Castle, DK-2920 Charlottenlund, Denmark

Abstract. The heterotrophic dinoflagellate *Noctiluca scintillans* has a negligible swimming ability and feeds predominantly on immobile prey. How, then, does it encounter prey? *Noctiluca scintillans* is positively buoyant and, therefore, we hypothesized that it intercepts prey particles during ascent and/or that microscale shear brings it into contact with prey. *Noctiluca scintillans* has a specific carbon content 1–2 orders of magnitude less than that typical for protists and, thus, an inflated volume. It also has a density slightly less than that of the ambient water and therefore ascends at high velocities (~1 m h^{-1}). In stagnant water, clearance rates of latex spheres (5–80 μm) increased approximately with prey particle size squared. This scaling is consistent with *N.scintillans* being an interception feeder. However, absolute clearance rates were substantially lower than those predicted by modeling *N.scintillans* both as a spherical and as a cylindrical collector. The latter model assumes that prey particles are collected on the string of mucus that may form at the tip of the tentacle. Feeding, growth and prey selection experiments all demonstrated that diatoms are cleared at substantially higher rates than latex beads and other phytoplankters, particularly dinoflagellates. We propose that diatoms stick more efficiently than latex beads to the mucus of *N.scintillans* and that dinoflagellates reduce fatal contact behaviorally. We conclude that *N.scintillans* is an interception feeder and that the high ascent velocity accounts for encounters with prey. However, the flow field around the cell–mucus complex is too complicated to be described accurately by simple geometric models. Fluid shear (0.7–1.8 s^{-1}) had a negative impact on feeding rates, which were much less than predicted by models. *Noctiluca scintillans* can survive starvation for long periods (>3 weeks), it can grow at low concentrations of prey (~15 μg C l^{-1}), but growth saturates only at very high prey concentrations of 500–1000 μg C l^{-1} or more. We demonstrate how the functional biology of *N.scintillans* is consistent with its spatial and seasonal distribution, which is characterized by persistence in the plankton, blooms in association with high concentrations of diatoms, and surface accumulation during quiescent periods or exponential decline in abundance with depth during periods of turbulent mixing.

Introduction

The dinoflagellate *Noctiluca scintillans* is common in temperate to tropical neritic waters around the world and is known at times to form pronounced red tides (Enomoto, 1956; Le Fèvre and Grall, 1970; Uhlig and Sahling, 1990). While the tropical form of the species may contain endosymbiontic algae (Sweeney, 1971), the temperate form is obligately heterotrophic. Field studies suggest that *N.scintillans* feeds mainly on immobile prey, particularly diatoms (Enomoto, 1956; Prasad, 1958). In accordance, laboratory studies have reported high growth rates on pure diets of diatoms (Buskey, 1995). Two different feeding behaviors have been qualitatively described in the literature: 'raptorial' feeding by individual cells and 'mucoid filtration' by groups of cells that scavenge particles during sinking (Omori and Hamner, 1982; Uhlig and Sahling, 1990; Shanks and Walters, 1996). In addition, Tiselius and Kiørboe (1998) described how *N.scintillans* colonize aggregates of diatoms to feed on them.

Noctiluca scintillans possesses a tentacle near the cytostome and a rudimentary flagellum (Lucas, 1982), neither of which serves motility function. Considering both the negligible swimming capacity of *N.scintillans* and its immobile prey, we

wondered how *N.scintillans* ever encounters prey. *Noctiluca scintillans* cells are normally positively buoyant (Kesseler, 1966) and thus ascend in the water column. For example, estimated collision rates between *N.scintillans* and diatom aggregates due to the rising of *N.scintillans* cells are sufficient to account for the colonization of diatom aggregates observed by Tiselius and Kiørboe (1998). Would a similar mechanism be sufficient to account for feeding on individual diatom cells? Or does microscale turbulence play a role for encountering food? In this study, we examine the functional biology of *N.scintillans*, with particular emphasis on the mechanism by which individual cells of *N.scintillans* encounter single food particles. We hypothesize that *N.scintillans* is an interception feeder that scavenges prey particles during ascent and/or that turbulent fluid shear brings *N.scintillans* in contact with its prey. We present simple models and results of laboratory experiments that aim to assess the significance of these two prey encounter mechanisms.

Prey encounter models

The rate at which a predator encounters prey, e, is given by (Kiørboe and Saiz, 1995):

$$e = \Sigma\beta_i C$$

where β_i are the kernels of the relevant encounter processes and C is the concentration of prey. $\Sigma\beta_i$ can thus be considered an estimate of the clearance rate. We here examine encounters by raptorially feeding cells due to (i) differential vertical velocity and (ii) turbulent shear. As a first approximation, we assume both *N.scintillans* and its prey to be spherical.

Differential vertical velocity

Several apparently conflicting geometric models describe particle encounter rates for translating spheres at low *Re*. Figure 1A describes schematically the flow lines around a translating sphere. Prey particles following streamlines within one particle radius from the collector are intercepted. One model, developed explicitly to describe prey encounter in suspension-feeding flagellates, simply estimates the clearance rate (β) as the volume flux through the annulus between the collector and the limiting streamline (Fenchel, 1984; Shimeta and Jumars, 1991):

$$\beta_{\Delta v} = (2\pi r_N r_P + \pi r_P^2)v \sim 2\pi r_N r_P v \qquad \text{for } r_P \ll r_N \qquad (1)$$

where v is the local (not far-field) fluid velocity, and r_N and r_P are the radii of the predator and the prey, respectively. This model predicts that clearance increases linearly with increasing size of both prey and predator (Fenchel, 1986a; Shimeta and Jumars, 1991). Classical coagulation theory (e.g. Hill, 1992) suggests a different model and estimates the encounter rate kernel as $\beta = 0.5\pi r_P^2 U$, where U is the (vertical) velocity difference between *N.scintillans* and its prey (~ascent

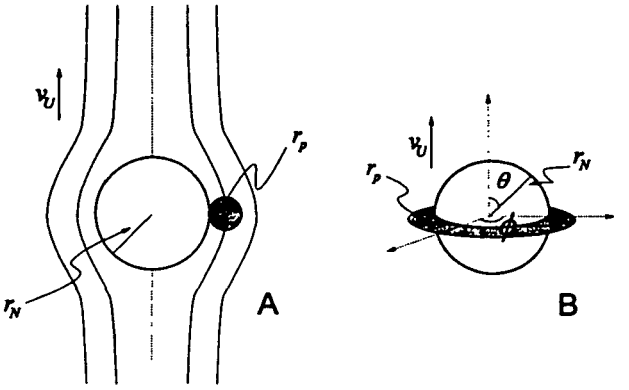

Fig. 1. Schematic of flow lines around a translating sphere with explanations of symbols used in the text.

velocity of *N.scintillans*). This model, somewhat counterintuitively, suggests that the clearance rate is independent of the predator size and scales only with the radius of the prey particle squared. Thus, the two models have fundamentally different implications to feeding rates and prey size spectra in interception feeders. They may reconcile, however, because v in equation (1) depends on the distance to the collector. Owing to the no-slip condition, the fluid velocity relative to the collector is zero right at its surface and increases asymptotically with increasing distance. The radial and azimuthal components of the fluid velocity relative to the translating sphere are, respectively (e.g. Berg, 1993):

$$v_r = -U\cos\theta(1 - 3r_N/2r + r_N^3/r^3) \tag{2}$$

and

$$v_\theta = U\sin\theta(1 - 3r_N/4r - r_N^3/4r^3) \tag{3}$$

where r is the distance to the center of the predator and θ the angle relative to the direction of the motion of the sphere (Figure 1B). The volume flux through the equatorial annulus can now be estimated as:

$$\beta_{\Delta v} = \int_0^{2\pi}\int_{r_N}^{r_N + r_p} r v_\theta\left(r, \frac{p}{2}\right) dr \cdot d\varphi = \pi U \cdot \frac{r_P^2(3r_N + 2r_P)}{2(r_N + r_P)}$$

$$\sim 1.5\pi U r_P^2 \qquad \text{for } r_P \ll r_N \tag{4}$$

This expression is identical to that cited by Spielman (1977) and, except for the lead coefficient, similar to that proposed by classical coagulation theory.

Turbulent shear

The diameters of both *N.scintillans* and its prey are well below the Kolmogorov scale for any realistic intensities of turbulence in the ocean. At these scales, turbulence is manifest as laminar shear, and can be quantified by a shear rate, γ. If shear is the only mechanism accounting for prey encounters, then (Hill, 1992):

$$\beta_{Shear} = 9.75\gamma(r_N + r_P)^3 (p^2/(1 + 2p)^2) \quad (5)$$

where $p = r_P/r_N$.

Method

Culture

Noctiluca scintillans (2000+ individuals) were collected in Gullmarsfjorden on the west coast of Sweden in October 1996. Cultures were established in 60–1000 ml screw-cap bottles containing 0.2-μm-filtered autoclaved sea water (30 p.p.t) and a mixture of phytoplankton (Table I) in total concentrations exceeding 10 p.p.m. The bottles were mounted on a slowly rotating wheel (0.2 r.p.m.) in a thermostated room (18°C) with a light:dark cycle of 16:8 h. All experiments were conducted at these temperature and light conditions. Cells were transferred to fresh food suspensions 2–3 times weekly. We aimed at culture concentrations of 1–10 cells ml^{-1}.

Carbon content

The carbon content of *N.scintillans* cells that had starved for 0, 1, 2 and 3 days was measured by an infrared gas analyzer. Batches of 100–300 cells were pipetted onto ashed 25 mm GF/C filters. Filters were then dried at 60°C for 2 h, and stored in an exicator at –20°C until analysis. Carbon content per cell was estimated as the slope of regressions of the total amount of carbon versus the number of cells per filter. Cell diameters of 50–200 cells were measured daily. Carbon contents of phytoplankton cells used as food were determined in a similar way, except that their sizes and concentrations were quantified by an electronic particle counter (ELZONE 180) (Table I).

Ingestion and clearance rates

To quantify ingestion and clearance rates in stagnant water, where ascent of *N.scintillans* is the presumed prey encounter mechanism, incubation bottles were placed on the plankton wheel. After a short spin-up time, water inside the bottle moves as a solid body (Jackson, 1994).

Ingestion rates were quantified by following the rate at which prey particles accumulated in the food vacuoles of *N.scintillans* incubated at known concentrations of particles. Clearance rates were estimated as the ingestion rate divided by ambient particle concentration. Food particles were either phytoplankton cells

Table I. Cell sizes and carbon content of phytoplankton species used as food in growth experiments and for cultivation of *N.scintillans*. Chain-forming species are marked with an asterisk

Species	Equivalent spherical diameter (μm)	Carbon content (μg C $μm^{-3}$) × 10^{-6}
Thalassiosira weisflogii	12.8	0.11
*Thalassiosira antarctica**	3.5	0.22
Ditylum brightwelli	21.2	0.037
*Skeletonema costatum**	8.13	0.16
*Chaetoceros affinis**	9.9	0.12
Prorocentrum minimum	9.8	0.12
Prorocentrum micans	22.0	0.30
Heterocapsa triqueter	16.1	0.13
Dunaliella marina	6.6	0.20
Rhodomonas baltica	6.2	0.21

(*Thalassiosira weisflogii* and *Heterocapsa triqueter*) or spherical latex beads of well-defined size (5, 9.9, 11.3, 16.3, 20.3, 40, 83 and 132 μm). In all experiments, *N.scintillans* were added to a concentration of ~1 ml^{-1} and prey particles to concentrations of <1 p.p.m. Incubations were conducted in 63 or (mainly) 270 ml tissue bottles, 1.2 l screw-cap bottles or in the Couette device (see below). When phytoplankton were used as food, *N.scintillans* had starved for 24 h prior to the experiment to void food vacuoles.

Up to 36 bottles for each prey size or type were started simultaneously. At intervals of 0.5–2 h, the contents of triplicate bottles were preserved with formalin. From each bottle, 50–300 cells were examined individually for food vacuole content. The 5 μm spheres could not be quantified in individual cells; instead, a known number of cells were sonicated, after which the destroyed cells and their food vacuole contents were allowed to settle. Prey particles were subsequently counted under an inverted microscope. These experiments confirmed that particle accumulation was approximately linear in time, and subsequent incubations were carried out with just one stop time.

Group feeding

To examine the potential advantages of 'group feeding', we incubated *N.scintillans* in concentrations of 0.1, 0.2, 0.4, 0.8 and 1.6 cells ml^{-1} in 625 ml bottles together with 20 μm latex beads. We examined food vacuole content in ~75 individuals per bottle (200–300 per treatment) after 7.5 h of incubation on the plankton wheel.

Particle size spectrum

Food size spectra were obtained by offering *N.scintillans* mixtures of latex beads in incubations lasting for ~18 h, and examining food vacuole content in sonicated cells as above. To avoid the total particle volume concentration exceeding 1 p.p.m. and to ensure a sufficient number of particles in suspension, particles were offered in the following four combinations: 5.0, 9.9, 16.5 and 20.3 μm; 9.9 and

40 μm; 9.9 and 83 μm; 9.9 and 132 μm. We had six bottles for each treatment. Relative size spectra were calculated by normalizing with the clearance on 9.9 μm particles.

Feeding in a Couette chamber

We examined the effect of fluid shear on prey encounter rates by comparing clearance rates on 40 mm particles in slowly rotating 1.2 l bottles (stagnant water) with clearance rates in a Couette flow. The latter was generated in a device which, briefly, consists of two cylinders, one inside the other. The outer cylinder rotates and thereby generates a well-defined fluid shear in the annular gap. Our Couettes were designed as described by Van Duuren (1968) and had a volume of 1.25 l. We conducted experiments at shear rates of 0.62 and 1.77 s^{-1}. Each experiment consisted of five Couettes and five rotating bottles, and lasted ~10 h. Food vacuole content was examined individually in >200 *N.scintillans* from each container.

Prey selection

Noctiluca scintillans collects prey particles in a clump of mucus on the tip of the tentacle. As a measure of prey 'selection', we quantified the frequencies of prey particles in the mucus relative to their frequencies in the ambient water. *Noctiluca scintillans* were incubated with *T.weisflogii* and one at a time the single-celled prey listed in Table I or 11.9 μm latex beads for 4–16 h in triplicate 63 ml culture flasks placed on a rotating wheel. Prey concentrations were 1000 ml^{-1} of each prey type. Prey frequencies in mucus were quantified by counting >200 prey particles per bottle.

The differential clearance rates on a diatom (*T.weisflogii*) and a dinoflagellate (*H.triqueter*) of similar size were examined by simultaneously incubating *N.scintillans* in pure suspensions and in mixtures of the two at identical number concentrations. We incubated five 270 ml bottles of each combination for 5 h and examined 15 cells from each bottle (i.e. 75 cells for each treatment) individually for food vacuole content.

Ascent rates and flow fields

To allow for interpretation of clearance rate observations, we examined ascent velocities of *N.scintillans* as well as the fluid flow around ascending cells. We measured ascent rates of *N.scintillans* that had starved for 0, 1, 2, 3 and 4 days. Individual *N.scintillans* cells were introduced into the lower third of a closed 5 × 5 × 20 cm^3 plastic aquarium which was submerged in a 10 l aquarium placed in a thermostated room. The cells were introduced with a few microliters of water via a pipette with a bent tip that was mounted in the lid of the inner aquarium. The size and movement of the cells were filmed with a CCD video camera with a 105 mm macro telephoto lens. Three–five tracks were recorded per cell, and average ascent rates were calculated for 10–20 cells per starving condition.

We used a similar set-up to quantify flow velocities past the equator of

ascending *N.scintillans* as a function of distance to the cell center. We estimated velocities of flow past six different ascending cells by tracking 15–60 neutrally buoyant particles (26 μm pollen grains) per cell. None of the cells had mucus attached. We plotted the positions of the particles relative to the cell on a plastic sheet at 0.5–1.0 s time intervals. For these experiments, the aquarium was placed on a stage, which could be moved in the X–Y plane, and the camera on a platform which could be moved vertically. This way, the ascending cell could be kept in exact focus in the middle of the screen at all times without focusing the lens and thereby changing the size calibration. The stage was equipped with meters that determined the position of the aquarium to within 20 μm. The depth of field of the pollen grains was determined to 1.0 mm. Because particles may be offset in the horizontal, apparent distances between the cell and particles, on average, slightly underestimate the true distance. By correcting with the depth of field (a), we converted apparent distances (d) to actual average distances (d_{avg}) by:

$$d_{avg} = \sqrt{\frac{a^2 + d^2}{2}} + \frac{d^2}{4} \ln\left[\frac{a + \sqrt{a^2 + d^2}}{-a + \sqrt{a^2 + d^2}}\right]$$

Growth

We examined the functional response in growth to variations in concentrations of a diatom (*T.weisflogii*) and a dinoflagellate (*H.triqueter*). Twenty cells were established in triplicate 63 ml tissue bottles with nominal concentrations of *T.weisflogii* or *H.triqueter* of 0, 0.3, 0.6, 0.9, 1.2, 1.8, 2.5, 5.0 or 10 p.p.m. An additional experiment was run with *H.triqueter* at nominal concentrations of 10, 20, 50 and 100 p.p.m. Bottles were mounted on the plankton wheel during incubations. To compensate for any potential effects of past food, the growth was followed for 4–7 days, and *N.scintillans* cells were counted and pipetted to fresh food suspension every 2 or 3 days. There were no time effects, though, and data were therefore pooled. Concentrations of phytoplankton food cells were measured on the electronic particle counter at the start and end of each incubation period. Growth rates were calculated as $\mu = \ln(C_{N,end}/C_{N,start})$, and average concentrations of food as $C_{P,avg} = (C_{P,end} - C_{P,start})/\ln(C_{P,end}/C_{P,start})$, where C denotes concentrations and subscripts refer to *N.scintillans* (N), phytoplankton food (P), and start, end and average concentrations. The diameters of 20 cells were measured at each food concentration at the end of the incubation. Additional growth experiments were conducted at a low (1.8 p.p.m.) and a high (18 p.p.m.) concentration of the diatoms and flagellate species listed in Table I.

Observations of feeding behavior

We observed behaviors of individual cells in dense suspensions of phytoplankton under a dissecting microscope.

Results

Feeding behavior

Noctiluca scintillans collects food particles by means of the ~300-μm-long tentacle which makes constant slow and asymmetrical movements. Prey cells may attach directly to the tip of the tentacle or become embedded in a clump or string of mucus that is attached to the tip of the tentacle. In dense suspensions of food, mucus strings ~100 μm broad and up to several millimeters long may form. Whereas *N.scintillans* cells without mucus appear to be randomly oriented in the water, cells with attached mucus are mainly oriented with the tentacle and mucus string downward. Before the actual ingestion, the mucus string is rolled into a clump of food particles at the tip of the tentacle and brought to the cytostome by the bending of the tentacle, whereupon it is phagocytized. This feeding mode is consistent with the observed frequency distribution of the numbers of prey in individual *N.scintillans* cells, which in all cases were significantly more clumped than a random (Poisson) distribution would predict. During incubations, *N.scintillans* were often seen in small aggregates.

Ascent rates, cell density, cell carbon and cell size

Cell motility relative to the surrounding water is due only to density differences between *N.scintillans* and the ambient water. All cells examined were positively buoyant, i.e. ascended in stagnant water. The ascent rates of individuals varied between ~0 and 1.7 m h^{-1}, but overall were positively correlated with cell size (Figure 2A). Ascent rates scaled approximately with cell diameter squared, which is consistent with Stokes' law. The density difference between the cells and ambient water ($\Delta\rho$, g cm^{-3}) was calculated from Stokes' law assuming spherical cell shape, $\Delta\rho = U/(21\,800r^2)$, where r is cell radius in centimeters and U is ascent velocity in centimeters per second. The average density difference was almost constant during the first 2 days of starvation, whereupon it increased slightly (Figure 2B). Thus, starved cells of set size ascend faster than well-fed cells.

Noctiluca scintillans cells contained ~0.2 μg C $cell^{-1}$, but the carbon content declined slightly during the 4 days of starvation (Figure 3A). The carbon to volume ratio of cells was very low, between 4.6 and 5.9 × 10^{-9} μg C μm^{-3}, and declined by ~20% during the 4 days of starvation (Figure 3B).

Cell size increased almost linearly with decreasing growth rate and cells swelled further during starvation (Figure 4). Since $U \sim \Delta\rho r^2$, the combined effect of variation in cell size and density with food condition implies a 3-fold average difference in ascent rates between starved and rapidly growing cells.

Ingestion and clearance rates in rotating bottles

Uptake of latex beads. In most cases, uptake of latex spheres increased linearly with time during the initial 12–15 h (Figure 5). In the experiment in which 40 μm sized beads were offered, there was an apparent time lag with an initial low

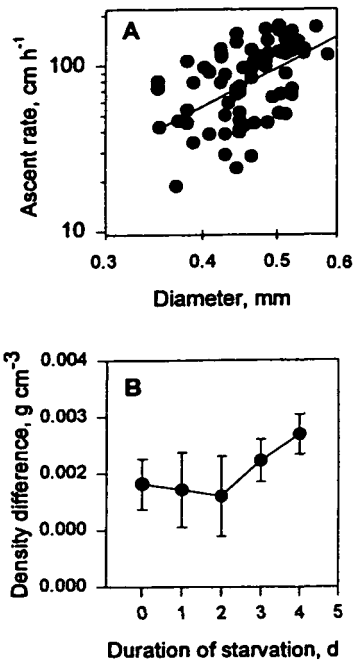

Fig. 2. *Noctiluca scintillans*. (**A**) Ascent velocity of individual cells as a function of cell size. The regression is statistically significant and has a slope of 2.4. (**B**) Density difference between ambient water and cells as calculated from Stokes' law.

uptake rate. Clearance rates increased with particle size: from 0.25 μl h^{-1} for 5 μm particles to 17.2 μl h^{-1} for 83 μm particles.

The rates at which latex beads were cleared and ingested were independent of the concentration of *N.scintillans* in the incubation container (Table II). Thus, there were no signs that group feeding enhanced clearance rates.

The particle size spectrum. The particle size spectrum, obtained as clearance rates relative to clearance of 9.9 μm sized particles in food mixture experiments, suggests an optimum prey particle size of ~80 μm (Figure 6A). Absolute clearance rates of latex spheres as a function of particle size, obtained from the time series experiments, were consistent with the left-hand side of the relative prey particle size spectrum (Figure 6B). Below the optimum prey particle size, clearance rate scaled with prey particle size to power 1.6, almost as predicted by equation (4). However, absolute clearance rates were higher than predicted. The slightly lower than predicted power of the scaling (2) may be caused by the larger particles approaching optimum particle size. Two observations on very small latex beads, that were calculated from Kirchner *et al.* (1996) and included in the plot, fit the pattern observed here.

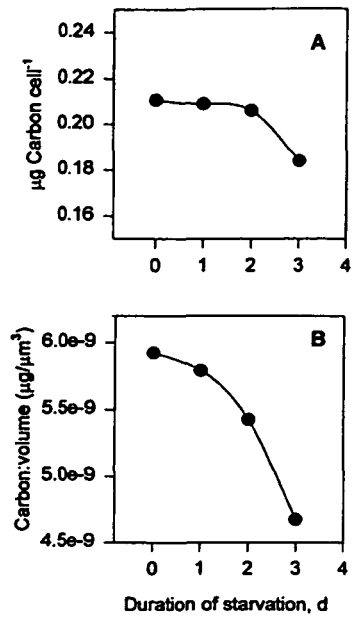

Fig. 3. *Noctiluca scintillans*. Carbon content per cell (**A**) and per unit volume (**B**).

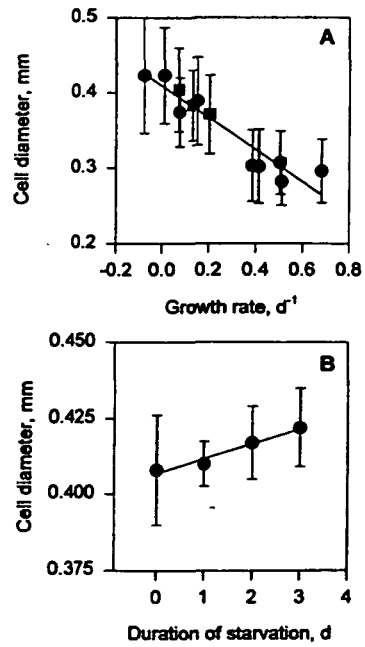

Fig. 4. *Noctiluca scintillans*. (**A**) Cell size (± SD) as a function of growth rate. Either *T.weisflogii* (circles) or *H.triqueter* (squares) were used as food. (**B**) Cell size (± SD) as a function of duration of starvation. Both regressions are statistically significant.

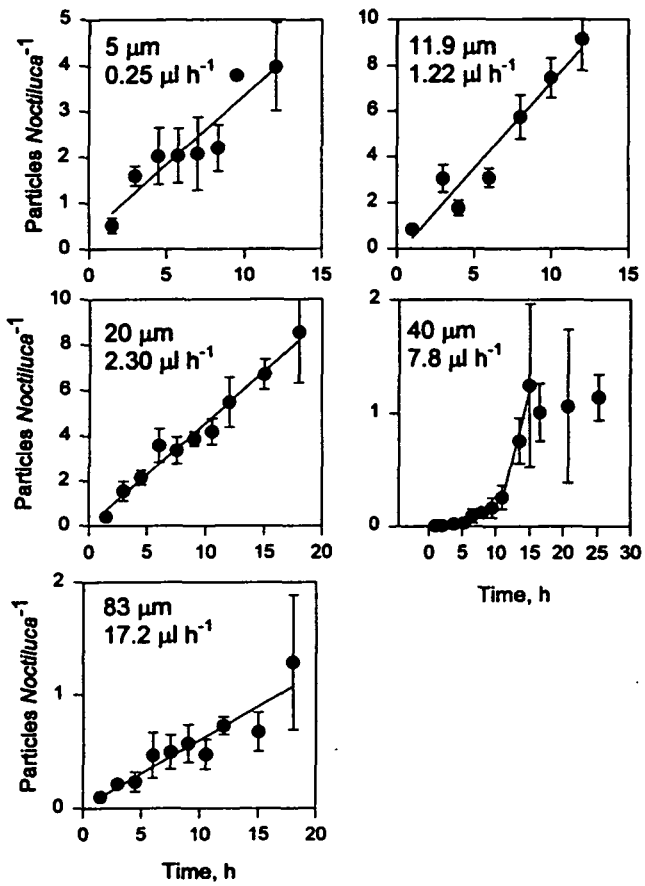

Fig. 5. *Noctiluca scintillans*. Accumulation of latex beads of various sizes in the food vacuoles of *N.scintillans*. Sizes of prey particles and calculated clearance rates (slopes of regressions divided by ambient particle concentration) are shown in the panels.

Table II. *Noctiluca scintillans*. Feeding rates on 20 µm latex beads (300 ml^{-1}) as a function of the concentration of *N.scintillans*

Concentration of *N.scintillans* (l^{-1})	Ingestion rate ± SD (beads ind.$^{-1}$ h^{-1})
0.1	1.34 ± 0.91
0.2	1.29 ± 0.04
0.4	1.49 ± 0.55
0.8	1.47 ± 1.20
1.6	1.34 ± 0.48

Prey selection and growth rates

Clearance rates on the diatom *T.weisflogii* were about one order of magnitude higher than those on the dinoflagellate *H.triqueter* (Table III). This difference

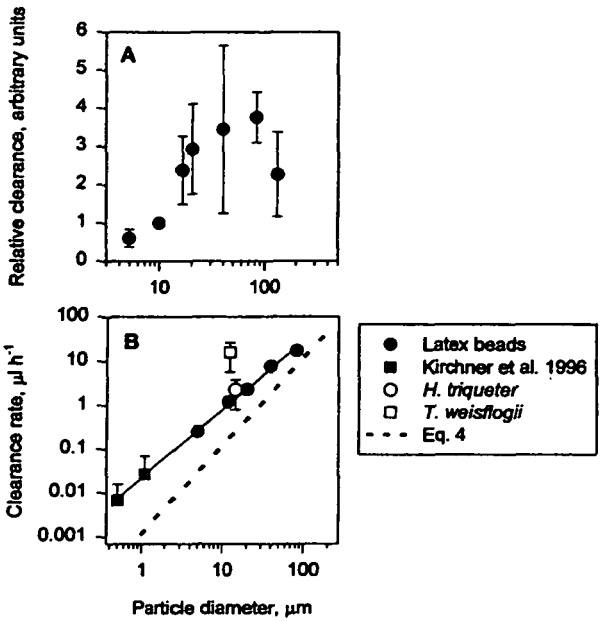

Fig. 6. *Noctiluca scintillans*. (**A**) Prey size spectrum. Data points are averages ± SD. (**B**) Clearance rates on latex beads (closed symbols) as a function of particle size. Two observations calculated from Kirchner *et al.* (1996) are also shown. The log–log regression (full line) has a slope of 1.6. The dotted line is the clearance predicted from equation (4) assuming an ascent velocity of 1 m h^{-1}. Average clearance rates on *T.weisflogii* and *H.triqueter* (open symbols) are also shown.

remains when the two species were offered in a mixture (Table IV). Also, in comparison to latex beads of similar size, the diatoms were cleared 10–25 times faster, while the dinoflagellates were cleared at similar rates as the beads (Figure 6B).

Relative frequencies of the different prey types collected in mucus normalized to the frequency of *T.weisflogii* also demonstrate significant prey selection (Table V). The different prey frequencies reflect different clearance rates, as demonstrated by the similar ratios of clearance rate and prey frequencies for both *H.triqueter* (0.126 versus 0.082) and 11.9 µm latex beads (0.127 versus 0.124). (The clearance ratios were calculated as the clearance of *H.triqueter* and latex beads, respectively, divided by the clearance of *T.weisflogii*; Table III and Figure 5.) The differences in prey frequencies are only partly due to different encounter probabilities related to size. When comparing with the size scaling factor obtained above, it is evident that *N.scintillans* collects dinoflagellates at lower rates than other cells (Table V). Thus, different particles of similar size are cleared with very different efficiencies.

Differences in growth rates on different diets further support the selection patterns. *Noctiluca scintillans* grows faster on, and growth saturates at a lower concentration of, the diatom *T.weisflogii* than on the dinoflagellate *H.triqueter* (Figure 7A and B). A comparison of the growth rates of *N.scintillans* offered a

Table III. *Noctiluca scintillans*. Summary of clearance rate measurements on phytoplankton estimated from accumulation rates of prey in food vacuoles

Species	Prey concentration (cells ml^{-1})	No. of replicates	R^2	Clearance (µl h^{-1})
Thalassiosira weisflogii	1186	5	0.92	12.6
	314	4	0.95	8.2
	614	4	0.91	9.4
	652	5	0.61	8.04
Average ± SD				9.6 ± 2.1
Heterocapsa triqueter	863	9	0.97	1.21

Table IV. *Noctiluca scintillans*. Clearance rates (µl h^{-1}; average and 95% confidence limits) on *T.weisflogii* and *H.triqueter* offered in pure and mixed suspensions. Prey concentrations were 300 ml^{-1} in all incubations

	Heterocapsa triqueter	*Thalassiosira weisflogii*
Pure suspension	3.31 ± 1.49	32.29 ± 17.13
Mixture	3.71 ± 1.67	22.76 ± 11.33

Table V. *Noctiluca scintillans*. Frequencies of various prey types collected in mucus relative to the frequency of *T.weisflogii*. The expected frequencies are calculated from the observed scaling between clearance rates and prey particle size

Particle type	Expected relative encounter probability from size (exponent 1.5)	Observed relative frequency of prey in mucus
Thalassiosira weisflogii	1.00	1.00
Ditylum brightwelli	2.13	1.33 ± 0.29
Prorocentrum minimum	0.67	0.060 ± 0.065
Prorocentrum micans	2.25	0.049 ± 0.001
Heterocapsa triqueter	1.41	0.082 ± 0.026
Dunaliella marina	0.37	0.35 ± 0.09
Rhodomonas baltica	0.34	0.18 ± 0.07
11.9 µm latex beads	–	0.124 ± 0.015

variety of phytoplankton suggests that, with the exception of *Chaetoceros affinis*, diatoms in general support higher growth rates than do flagellates (Figure 7C). Unsaturated growth rates on the different prey species normalized to growth on *T.weisflogii* correlate well with the relative frequencies of prey collected in mucus for solitary species (Figure 8). This demonstrates that variation in growth is due mainly to *N.scintillans'* variable capability to capture different types of prey, rather than to differences in the nutritional quality of the different prey species.

Particle clearance in Couette flow

In both of the two experiments conducted, clearance rates in the Couette flow were lower than in the rotating bottles ($P < 5\%$; Table VI). Clearance rates were

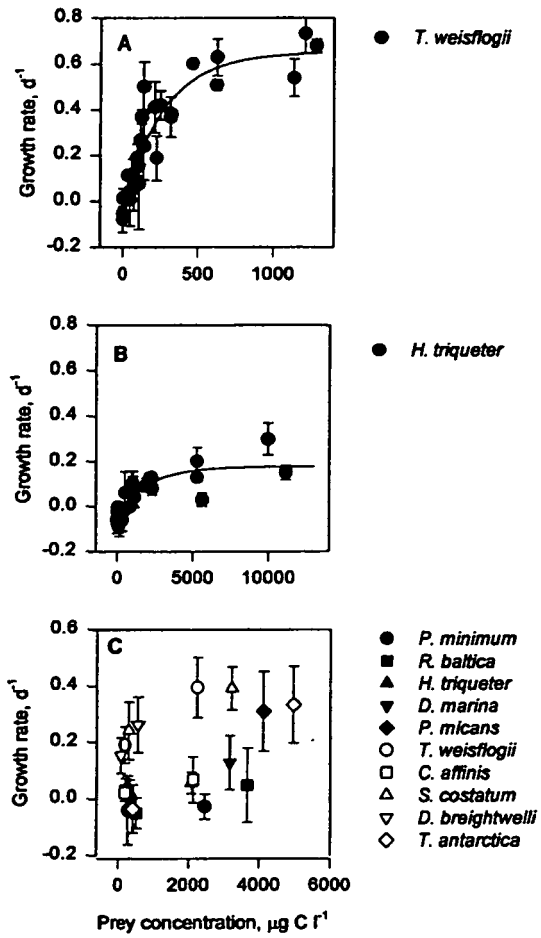

Fig. 7. *Noctiluca scintillans*. Functional response in growth rate to variations in prey concentration and prey species. In (**A**) (*T.weisflogii*) and (**B**) (*H.triqueter*), the data were fitted to $\mu = K(1 - e^{-aC}) - b$, where μ is the specific growth rate, C is the concentration of prey, and K, a and b are constants. The fitted parameters yield estimated maximum growth rates ($K - b$) of 0.63 and 0.18 day^{-1} for the diatom and the dinoflagellate prey, respectively. A total of 90% of maximum growth [$-\ln(0.1 - 0.1b/K)/a$] was achieved at 5.8 and 38.8 p.p.m. (**C**) Growth rates on a variety of diatom (open symbols) and flagellate (closed symbols) prey species.

also considerably lower than predicted from considering shear as the sole prey encounter mechanism [cf. equation (5)]. Apparently, shear of the magnitude used here does not enhance the ingestion rate in *N.scintillans*.

Flow field

The flow velocity data were pooled after normalizing with size and ascent velocity of individual cells, and then compared with the prediction from equation (3)

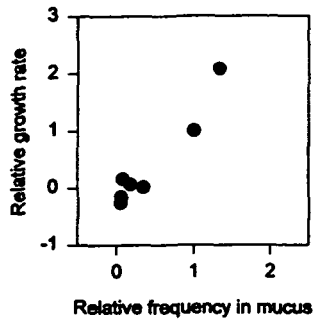

Fig. 8. *Noctiluca scintillans*. Growth rates on various single-celled phytoplankton species (normalized by the growth on *T.weisflogii* and corrected for variations in prey concentration) versus relative frequencies of the same prey species collected in mucus (from Table V).

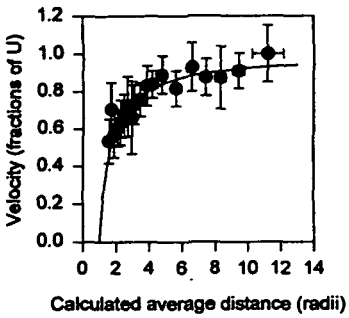

Fig. 9. *Noctiluca scintillans*. Flow velocities past the equator of ascending cells as a function of the calculated average distance to the cell center. Measurements on different cells were normalized by ascent velocity (U) and radius. The line is that predicted by theory [equation (3)].

Table VI. *Noctiluca scintillans*. Clearances rates ± SD of 40 μm latex beads (≤30 ml^{-1}) in sheared flow (Couette device). Expected clearance rates are calculated from equation (5). Simultaneous incubations in rotating bottles served as controls

Experiment no.	Shear rate (s^{-1})	Expected clearance (μl h^{-1})	Observed clearance (μl h^{-1})	Control clearance (μl h^{-1})
1	0.62	1.60	0.57 ± 0.18	2.74 ± 0.92
2	1.77	4.32	0.67 ± 0.24	4.32 ± 0.44

(Figure 9). Despite the fact that *N.scintillans* is not perfectly spherical, the observed fluid velocities were almost identical to those predicted.

Discussion

Prey encounter mechanisms

Clearances and ingestion rates provide conservative estimates of prey encounter rates, because not all particles encountered are necessarily captured and

subsequently ingested. In spite of this, observed clearance rates of *N.scintillans* in stagnant water were significantly higher than those predicted from simple geometric considerations [equation (4)]. This was particularly so in the case of the diatom *T.weisflogii*, which was cleared 1–2 orders of magnitude faster than expected. Similar high clearance rates can be derived for *T.weisflogii* and *H.triqueter* from the functional responses in growth rate to food concentration by assuming a growth efficiency of 0.33 (Hansen *et al.*, 1997). Such calculations yield 35 and 2.5 μl ind.$^{-1}$ h^{-1} on *T.weisflogii* and *H.triqueter*, respectively. Tiselius and Kiørboe (1998) reported clearance rates on ~30 μm diatoms of 10–20 μl h^{-1}, which are also some 10–20 times higher than predicted. The prey selection experiments suggest that other phytoplankters, particularly diatoms, were also cleared at higher rates than expected. Observations of the actual flow field around ascending cells did not help explain this discrepancy because flow velocities increased with distance from the ascending cell almost exactly as assumed in our model.

There may be several reasons for the discrepancy between observed and expected clearance rates. The assumption of a spherical collector is a first approximation, but may be too simplistic. First, *N.scintillans* cells were at times observed in groups or aggregates, similar to but denser than the feeding associations described by Uhlig (1983) in the laboratory and by Shanks and Walters (1996) in the field. Shanks and Walters (1996) found that *N.scintillans* in aggregates had higher food vacuole content than solitary cells and, thus, presumably higher feeding rates. Because ascent rate scales with $R^2\Delta\delta$ (Stokes' law), groups of cells may experience higher ascent rates than individual cells and thus clear larger volumes of water (R = equivalent spherical radius of an aggregate). However, particles in this larger volume of water are to be shared by more individuals. If the porosity (fractional water content) of a group of cells is Po, then the density difference between the aggregate and ambient water is $\Delta\delta = (1 - Po)(\delta_C - \delta_W)$, where δ_C and δ_W are the densities of cells and water, respectively. Because $R^2(Po,n) = r^2n^{2/3}(1 - Po)^{-2/3}$, per capita clearance rates scale with $R^2\Delta\delta/n = (1 - Po)^{1/3}(\delta_C - \delta_W)r^2n^{2/3}$, where n denotes the number of individuals in an aggregate. Thus, per capita clearance rates would be lower rather than higher in aggregated cells and would decline with aggregate size (n). This formulation assumes no flow of water through the aggregate. However, intra-aggregate flow, which might increase encounter volume, is likely very limited due to the presence of mucus binding the cells together in the aggregate. Accordingly, the experiments in which the concentration of *N.scintillans*, and hence the ability to form aggregates, was varied, did not show higher clearance rates when *N.scintillans* occurred in high concentrations (Table II).

Flow fields were only determined around cells with little or no mucus. However, the mucus strings attached to the tentacle can at times be quite impressive. Thus, the cell–mucus complex is far from being spherical, even in solitary *N.scintillans*. Also, prey are collected on the tentacle or in the mucus, rather than by interception on the cell body. Therefore, a cylindrical rather than a spherical collector might provide a better model of prey capture in *N.scintillans*. From Spielman (1977), we derive an approximate expression for the encounter rate kernel for a cylindrical collector (β_{Cyl}):

$$\beta_{Cyl} = 4A_F l \cdot \frac{r_P^2}{r_M} w \quad (6)$$

where r_M is the radius of the mucus string, l its length, w the component of the far-field velocity which is perpendicular to the mucus string, and $A_F \sim 0.1$ for $Re \sim 0.01$–0.1 (which is representative). If we assume $l = 0.3$ cm (about the longest threads seen), $r_M = 0.005$ cm (typical) and $w = 100$ cm h^{-1}, then 10 μm particles will be cleared at ~5 μl h^{-1}. This is the right order of magnitude. Thinner threads yield higher clearance rates, because the encounter rate kernel [equation (6)] scales inversely with the thickness of the thread. However, mucus threads were usually not oriented perpendicular to the flow, but rather aligned with the flow. Therefore, w in equation (6) is typically much lower than the ascent velocity. (In a rotating bottle, mucus threads will tend to be oriented downward and thus experience flow past it as the *N.scintillans* rotates with the fluid.) A cylindrical collector mechanism can, therefore, not fully account for the observed magnitude of the clearance rates either. Thus, our modeling attempts can predict observed clearance rates only to within one order of magnitude or so. We conclude that although the ascent of *N.scintillans* is the mechanism which generates the velocity difference between *N.scintillans* and its prey, the (variable) shape of the collector and the exact flow patterns are too complicated to be modeled realistically.

Both models [equations (4) and (6)] propose that $\beta \sim r_P^2$, which is almost as observed. This prediction is independent of the shape of both the collector and of the detailed flow field and, thus, generally true for interception feeding on small particles. The flow velocity past á solid surface initially increases almost proportionally with the distance to the surface. Therefore, the volume flow through an area perpendicular to the solid surface and delimited by the streamline at distance r_p is $\sim r_P v \sim r_p^2$. Because the observed clearance rates scale approximately as predicted, we conclude that *N.scintillans* collects prey particles by direct interception.

Prey capture rates in a sheared flow were substantially lower than those expected from equation (5), and also lower than those in stagnant water (Table VI). If shear had no effect, we would expect similar prey capture rates in stagnant water and sheared flow because prey scavenging by ascent would still occur in the Couette device. Deleterious effects of shear on dinoflagellates have previously been reported (Thomas and Gibson, 1990, 1992). In the present case, shear may simply destroy the *N.scintillans*–mucus complex and thereby interfere with the feeding process. Typical energy dissipation rates (ε) in the upper ocean range from 10^{-5} to 10^{-1} cm^3 s^{-2} (Kiørboe and Saiz, 1995). Microscale shear relates to energy dissipation rate as $\gamma = (\varepsilon/\nu)^{0.5}$, where ν is the kinematic viscosity (~10^{-2} cm^2 s^{-1}). Representative dissipation rates are, thus, 0.03 and up to 3 s^{-1}. Although within that range, shear rates of 0.7 and 1.7 s^{-1} as used here are only experienced by *N.scintillans* during quite windy conditions.

Prey selection

Prey selection and growth experiments suggest that different particles are cleared at different rates, also when offered in mixtures, and even when differences in size are accounted for. Despite their own motility, which would increase encounter rates, dinoflagellates are cleared at substantially lower rates than are immobile diatoms. However, dinoflagellates are capable of avoiding fatal contact. We frequently observed that *H.triqueter*, for example, upon swimming into a mucus thread, tumbled and continued swimming away from the mucus thread and, thus, avoided becoming entangled. It is more difficult to explain the substantial difference in clearance rates between *T.weisflogii* and similarly sized latex beads. 'Active' prey selection, based on chemical or other cues, is difficult to envisage, given the nature of the prey capture mechanism. However, phytoplankton cells, particularly diatoms, are known to be 'sticky', i.e. to adhere upon contact (e.g. Kiørboe and Hansen, 1993). The exact mechanism of sticking is unknown, but is probably related to mucus secretion (Kiørboe and Hansen, 1993; Waite *et al.*, 1995) which is known to be copious in diatoms (Decho, 1990). This suggests that, once encountered, sticky diatoms are captured with greater efficiency than latex beads.

Significance of size

Noctiluca scintillans is an unusual dinoflagellate in several ways. Most conspicuous are its size and inflated volume. The volume-specific carbon content of *N.scintillans* is almost two orders of magnitude less than that typical of other protists, including dinoflagellates, which have carbon to volume ratios of the order of 1–2 $\times 10^{-7}$ μg C μm^{-3} (Hansen *et al.*, 1997). The cell size of *N.scintillans* increases with decreasing food availability and the cells swell further upon starvation (Figure 4) (Buskey, 1995). This is in contrast to other dinoflagellates—and protists in general (Fenchel, 1986a)—which show the opposite and more expected response (Hansen, 1992; Jacobsen and Anderson, 1993; Jakobsen and Hansen, 1997).

What, if any, is the functional significance of the inflated volume of *N.scintillans*? The encounter rate formulation of Shimeta and Jumars (1991) [equation (1)] suggests that larger cells may intercept more prey particles, but we have argued above that this is not the case. Instead, we propose that the inflated size of *N.scintillans* may represent an adaptation to enhance its ascent rate and, thereby, its prey encounter rate. Had *N.scintillans* had a size corresponding to its carbon content, and because ascent velocity scales with the square of the radius, it would ascend at rates about an order of magnitude slower than it actually does. Such low ascent rates would, in turn, imply an order of magnitude lower prey capture rates. The variation in size and density (Figure 2) with food availability further implies that starved cells may ascend three times faster than well-fed cells. The unusual response in cell size to food availability may be interpreted in this light.

The volume-specific clearance rate of interception feeding flagellates scales with r_P^2/r_N^3, and therefore decreases much faster with size than other vital rates.

Such a scaling argument led Fenchel (1986a) to suggest that the efficiency of interception feeding is severely limited by size and is, therefore, expected to occur mainly among very small organisms, such as heterotrophic flagellates. We have argued that *N.scintillans*, in spite of its considerable size, is an interception feeder. Typical predator to prey size ratios in protozoa are 10:1 or higher (Fenchel, 1986b). The size ratio of *N.scintillans* to its optimum prey is ~4:1. If the size of *N.scintillans* is corrected for its high water content, the ratio would approach 1:1. Thus, *N.scintillans* feeds preferentially on prey with a dry mass similar to its own. Such relatively large optimum prey sizes are also found in other heterotrophic dinoflagellates (Hansen, 1992; Jakobsen and Hansen, 1997). The scaling of the efficiency of interception feeding with prey size squared may partially compensate for the low efficiency related to being large. Yet, the clearance rate of *N.scintillans* seems low in comparison to those of other zooplankters. The specific clearance on prey of optimum size and type is ~3×10^2 body volumes h^{-1}, which is about two orders of magnitude less than that predicted by the general size relationship for zooplankters, including dinoflagellates, compiled by Hansen *et al.* (1997). If one corrects for the inflated body volume of *N.scintillans*, the maximum clearance becomes within one order of magnitude of that predicted, but is still in the lower end.

Seasonal and vertical distribution of N.scintillans

Our observations on the functional biology of *N.scintillans* may help explain some characteristics of its seasonal and spatial occurrence. During calm periods and in fronts associated with convergence zones, 'blooms' of *N.scintillans* often conclude in dense accumulations of cells at the surface, causing discoloration of the water (Le Fèvre and Grall, 1970). The positive buoyancy of the cells facilitates the accumulation. However, normally turbulent mixing is sufficient to prevent surface accumulation. At steady state, the constant ascent of cells will be balanced by vertical mixing according to $K(dC_Z/dz) + UC_Z = 0 \Rightarrow C_Z = C_0 e^{-(U/K)Z}$, where K is the eddy diffusivity, C_Z is the concentration of cells at depth z and U the ascent velocity of the cells. Thus, with constant K, cell concentration should decline exponentially with depth. This prediction is borne out by observational data [Figure 10; data from Painting *et al.* (1993) and Kimor (1979); see also Uhlig and Sahling (1990)]. The magnitudes of the eddy diffusivities, estimated from the vertical distribution by assuming $U = 1$ m h^{-1}, are consistent with those typical for the upper ocean (~10^{-1}–10^{-3} m^2 s^{-1}; Sundby, 1997). On cessation of wind and, hence, turbulent mixing, K tends to zero and cells may accumulate at the surface. Surface accumulation may be fatal to the cells because it prevents continued ascent and, hence, feeding. Accordingly, Uhlig and Sahling (1990) reported that cells in such surface slicks had little food vacuole content and were in poor condition. Thus, although our experiments suggest that too high turbulence may be detrimental to the feeding process, *N.scintillans* apparently requires some intermediate level of turbulence to avoid surface accumulation.

The vertical distribution of *N.scintillans* may at times deviate significantly from the expected exponential decline with depth. Kiørboe *et al.* (1998) and Omori and

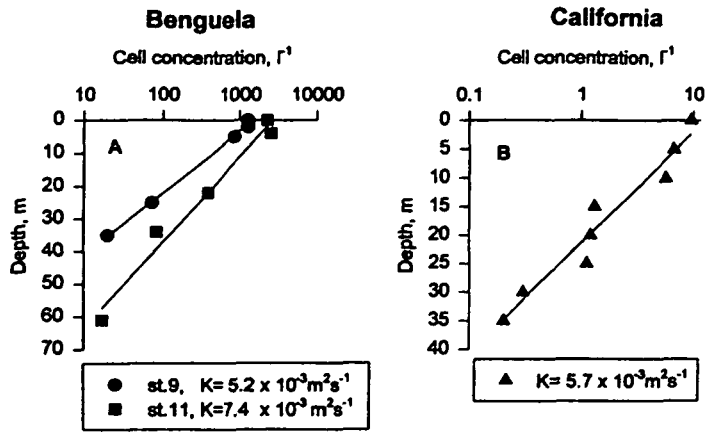

Fig. 10. Vertical distribution patterns of *N.scintillans* at selected stations in (**A**) an upwelling plume in the southern Benguela in March 1983 and (**B**) off southern California on 20 March 1976; data from Painting *et al.* (1993) and Kimor (1979), respectively. Coefficients of vertical eddy diffusivity (*K*) were calculated assuming an ascent rate of 100 cm h^{-1} in all cases.

Hamner (1982) both observed significant subsurface accumulations of *N.scintillans*. In these cases, *in situ* observations revealed that *N.scintillans* cells had colonized diatom aggregates and, respectively, were tethered to particle-loaded mucus strings and to each other. Such feeding-related behaviors result in the anchoring of *N.scintillans* at depth. It is unclear what environmental factors result in solitary versus aggregation or group feeding behavior and, hence, in the very different vertical distribution patterns.

Noctiluca scintillans occurs in the plankton throughout the year at low concentrations, also when food is sparse (Uhlig and Sahling, 1990). Occasionally, elevated growth concludes in mass occurrence and red tide. While the clearance rate of *N.scintillans* appears to be substantially lower than that of similar sized zooplankters, its maximum growth rate is similar or even higher than that predicted by a general relationship between growth rate and size in zooplankters, including dinoflagellates (Hansen *et al.*, 1997). However, *N.scintillans* achieves high growth only at very high prey concentrations, and growth saturates at concentrations exceeding 500–1000 μg C l^{-1} (Figure 7A) or more (Figure 7B and C). Such concentrations are representative of phytoplankton blooms. The high food concentration required for excessive growth, and the passive selection of diatoms, may account for the numerous reports of high concentrations of *N.scintillans* associated with diatom blooms (Enomoto, 1956; Prasad, 1958; Schaumann *et al.*, 1988; Painting *et al.*, 1993; Kiørboe *et al.*, 1998). On the other hand, *N.scintillans* can survive without food for periods exceeding 3 weeks (own unpublished observations; Buskey *et al.*, 1992) and requires a threshold of only 15 μg C l^{-1} (*T.weisflogii*; Figure 7A) to maintain positive growth. The formation of swarmers may further prolong the survival period. In conjunction, these features allow *N.scintillans* both to persist in the plankton during periods of low

food availability and to take advantage of diatom outbursts of limited spatial and temporal duration.

Acknowledgements

This work was supported by a grant from the Danish Natural Science Research Council (#9502163) to T.K. and a NorFA fellowship (#96.30.212-O and 96.30.236-O) to J.T. A.Visser advised on modeling aspects and J.Melbye, L.Christensen and J.Christensen provided technical assistance.

References

Berg,H.C. (1993) *Random Walks in Biology*, 2nd edn. Princeton University Press, New Jersey, 152 pp.

Buskey,E.J. (1995) Growth and bioluminescence of *Noctiluca scintillans* on varying algal diets. *J. Plankton Res.*, **17**, 29–40.

Buskey,E.J., Strom,S. and Coulter,C. (1992) Bioluminescence of heterotrophic dinoflagellates from Texas coastal waters. *J. Exp. Mar. Biol. Ecol.*, **159**, 37–49.

Decho,A.W. (1990) Microbial exopolymer secretions in ocean environments: their role(s) in food web and marine processes. *Oceanogr. Mar. Biol. Annu. Rev.*, **28**, 73–153.

Enomoto,Y. (1956) On the occurrence and the food of *Noctiluca scintillans* (Macartney) in the waters adjacent to the west coast of Kyushu, with special reference to the possibility of the damage caused to the fish eggs by that plankton. *Bull. Jpn. Soc. Sci. Fish.*, **22**, 82–88.

Fenchel,T. (1984) Suspended marine bacteria as a food source. In Fasham,M.J. (ed.), *Flow of Energy and Materials in Marine Ecosystems*. Plenum Press, New York, pp. 301–314.

Fenchel,T. (1986a) The ecology of heterotrophic microflagellates. *Adv. Microb. Ecol.*, **9**, 57–97.

Fenchel,T. (1986b) Protozoan filter feeding. *Prog. Protistol.*, **1**, 65–113.

Hansen,P.J. (1992) Prey size selection, feeding rates and growth dynamics of heterotrophic dinoflagellates with special emphasis on *Gyrodinium spirale*. *Mar. Biol.*, **114**, 327–334.

Hansen,P.J., Bjørnsen,P.K. and Hansen,B.W. (1997) Zooplankton grazing and growth: Scaling within the 2–2000 mm body size range. *Limnol. Oceanogr.*, **42**, 687–704.

Hill,P.S. (1992) Reconciling aggregation theory with observed vertical fluxes following phytoplankton blooms. *J. Geophys. Res.*, **97**, 2295–2308.

Jacobsen,D.M. and Anderson,D.M. (1993) Growth and grazing rates of *Protoperidinium hirobis* Abé, a thecate heterotrophic dinoflagellate. *J. Plankton Res.*, **15**, 723–736.

Jakobsen,H.H. and Hansen,P.J. (1997) Prey size selection, grazing and growth of the small heterotrophic dinoflagellate *Gymnodinium* sp. and the ciliate *Balanion comatum*—a comparative study. *Mar. Ecol. Prog. Ser.*, **158**, 75–86.

Kesseler,H. (1966) Beitrag zur Kenntnis der chemischen und physikalischen Eigenschaften des Zellsaftes von *Noctiluca miliaris*. *Veroff. Inst. Meeresforsch. Bremerh. Sonderband*, **2**, 357–368.

Kimor,B. (1979) Predation by *Noctiluca miliaris* Suriray on *Acartia tonsa* Dana eggs in the inshore waters of southern California. *Limnol. Oceanogr.*, **24**, 568–572.

Kiørboe,T. and Hansen,J.L.S. (1993) Phytoplankton aggregate formation: observations of patterns and mechanisms of cell sticking and the significance of exopolymeric material. *J. Plankton Res.*, **15**, 993–1018.

Kiørboe,T. and Saiz,E. (1995) Planktivorous feeding in calm and turbulent environments, with emphasis on copepods. *Mar. Ecol. Prog. Ser.*, **122**, 135–145.

Kiørboe,T., Tiselius,P., Michell-Innes,B., Hansen,J.L.S., Visser,A.W. and Mari,X. (1998) Intensive aggregate formation but low vertical flux during an upwelling induced diatom bloom. *Limnol. Oceanogr.*, **43**, 104–116.

Le Fèvre,J. and Grall,J.R. (1970) On the relationships of *Noctiluca* swarming off the western coast of Brittany with hydrological features and plankton characteristics of the environment. *J. Exp. Mar. Biol. Ecol.*, **4**, 287–306.

Lucas,I.A.N. (1982) Observations on *Noctiluca scintillans* Macartney (Ehrenb.) (Dinophyceae) with notes on an intracellular bacterium. *J. Plankton Res.*, **4**, 401–409.

Omori,M. and Hamner,W.M. (1982) Patchy distribution of zooplankton: behavior, population assessment and sampling problems. *Mar. Biol.*, **72**, 193–200.

Painting,S.J., Lucas,M.I., Peterson,W.T., Brown,P.C., Hutchings,L. and Mitchell-Innes,B.A. (1993) Dynamics of bacterioplankton, phytoplankton and mesozooplankton communities during the development of an upwelling plume in the southern Benguela. *Mar. Ecol. Prog. Ser.*, **100**, 35–53.

Prasad,R. (1958) A note on the occurrence and feeding habits of *Noctiluca* and their effects on the plankton community and fisheries. *Proc. Indian Acad. Sci. Sect. B*, **47**, 331–337.

Schaumann,K., Gerdes,D. and Hesse,K.-J. (1988) Hydrographic and biological characteristics of a *Noctiluca scintillans* red tide in the German Bight, 1984. *Meeresforschung*, **32**, 77–91.

Shanks,A. and Walters,K. (1996) Feeding by a heterotrophic dinoflagellate (*Noctiluca scintillans*) in marine snow. *Limnol. Oceanogr.*, **41**, 177–181.

Shimeta,J. and Jumars,P.A. (1991) Physical mechanisms and rates of particle capture by suspension feeders. *Oceanogr. Mar. Biol. Annu. Rev.*, **29**, 191–267.

Spielman,L.A. (1977) Particle capture from low-speed laminar flows. *Annu. Rev. Fluid Mech.*, **9**, 297–319.

Sundby,S. (1997) Turbulence and ichthyoplankton: influence on vertical distributions and encounter rates. *Sci. Mar.*, **61**, 159–176.

Sweeney,B.M. (1971) Laboratory studies of a green *Noctiluca* from New Guinea. *J. Phycol.*, **7**, 53–58.

Thomas,W.H. and Gibson,C.H. (1990) Quantified small-scale turbulence inhibits a red tide dinoflagellate, *Gonyaulax polyedra* Stein. *Deep-Sea Res.*, **3**, 1583–1593.

Thomas,W.H. and Gibson,C.H. (1992) Effects of quantified small-scale turbulence on the dinoflagellate, *Gymnodinium sanguineum (spendens)*: contrast with *Gonyaulax (Lingulodinium) polyedra* and fishery implication. *Deep-Sea Res.*, **39**, 1429–1437.

Tiselius,P. and Kiørboe,T. (1998) Colonization of diatom aggregates by the dinoflagellate *Noctiluca scintillans*. *Limnol. Oceanogr.*, **43**, 154–159.

Uhlig,G. (1983) *Biologische Anstalt Helgoland*. Jahresbericht, Hamburg, pp. 44–48.

Uhlig,G. and Sahling,G. (1990) Long-term studies on *Noctiluca scintillans* in the German Bight. Population dynamics and red tide phenomena 1968–1988. *Neth. J. Sea Res.*, **25**, 101–112.

van Duuren,F.A. (1968) Defined velocity gradient model flocculator. *J. Sanit. Eng. Div. Proc. Am. Soc. Civ. Eng.*, **94** no.SA4, 671–682.

Waite,A.M., Olson,R.J., Dam,H.G. and Passow,U. (1995) Sugar-containing compounds on the cell surfaces of marine diatoms measured using concanavalin A and flow cytometry. *J. Phycol.*, **31**, 925–933.

Received on December 28, 1997; accepted on April 16, 1998